NUMERICAL SIMULATION OF WAX DEPOSITION IN CHANNEL FLOW

Luis Renato Minchola Morán, luisminchola@mec.puc-rio.br
Angela Ourivio Nieckele, nieckele@mec.puc-rio.br
Luis Fernando Alzuguir Azevedo, lfaa@mec.puc-rio.br
Departamento de Engenharia Mecânica – Pontifícia Universidade Católica de Rio de Janeiro, PUC-Rio
R. Marques de São Vicente 225 – Rio de Janeiro, RJ, Brasil

Abstract. *Wax deposition continues to be a critical operational problem in crude oil carrying pipelines operating in cold environments. Therefore, accurate prediction of wax deposition rates and deposited wax spatial distribution is an invaluable information for the design of subsea lines. Unfortunately wax deposition is a complex process for which the mechanisms are still not fully understood. The present paper is part of a research program developed with the objective of identifying the relative importance of the different wax deposition mechanisms proposed in the literature. To this end, a two dimensional mathematical model was developed considering molecular diffusion as the only deposition mechanism. The mass, momentum, energy and wax concentration conservation equations were numerically solved with the Finite Volume Method. A non-orthogonal moving coordinate system that adapts to the wax interface deposit geometry wax employed. A simple laminar channel flow geometry was modeled and the results obtained compared with detailed experimental data available. The comparison between measured and predicted deposition profiles revealed discrepancies between transient deposition profiles, although the steady state deposition was reasonable predicted. Regions of sub-cooled fluid were identified in the numerical results and linked to the possibility of generating wax crystals that could contribute to the deposited layer by a Brownian- diffusion-based mechanism.*

Keywords*: wax deposition, pipeline, molecular diffusion, simulation.*

1. INTRODUCTION

Deposition of heavy paraffin molecules in the inner walls of pipelines is a relevant problem for the petroleum industry due to the potential capital losses that it imposes to the operators. Indeed, paraffin deposition may lead to loss of production, increased pumping power, elevated remediation costs and even loss of pipelines due to its total blockage. It is for that reason that there is a significant amount of publications with attempts of modeling this phenomenon. Most operator companies use simulation tools to predict the rate of wax deposition in pipelines. These models are employed in the design stages of the oil fields where the knowledge of the likelihood of occurrence of wax deposition is fundamental information that will influence the characteristics of the pipelines to be specified and, at the end, the cost of the future installation. Due to the complexity of the phenomena controlling the deposition of paraffin, the simulation models make use of empirical constants and correction factors that tune the model to particular field data. If, in one hand, this approach produces reasonable results that can be used in studies of the particular field from which the data were obtained, in the other hand it limits the applicability of the model to other fields with different characteristics, since the fundamental physics behind the deposition phenomena is not properly modeled. Studies of simpler configurations with simple oil-wax solutions provide valuable information that may help understand the underlying physics behind the paraffin deposition phenomenon.

The present paper is part of an ongoing research effort directed at identifying the relative importance of the mechanisms responsible for paraffin deposition. The research program encompasses experiments at the laboratory scale and numerical simulations. The experiments employ simple geometries with well defined and controlled boundary and initial conditions, using simple oil-paraffin solutions prepared in the laboratory, and with known transport properties. The results obtained from these controlled experiments are then compared to numerical simulations that try to faithfully reproduce the experimental conditions. Contrary to the experimental studies, the simulations studies permit that different models proposed for deposition mentioned in the literature can be tested individually, allowing, thereby, an assessment of the relative importance of each of the deposition mechanisms.

In previous papers (Romero et al., 2006), the same strategy described above was employed to assess the importance of molecular diffusion of liquid paraffin in solution as a possible deposition mechanism. Molecular diffusion has been used as a deposition mechanism in the vast majority of the simulations available in the literature (e.g., Brown at al., 1993, Fusi, 2003). However, as commented in (Leiroz, 2004), there is still controversy related to the relevance of other deposition mechanisms based on the lateral transport of solid paraffin crystal, such as Brownian diffusion and shear dispersion.

The present paper is a continuation of the work of Romero et al., 2006 In that work, a molecular-diffusion-based mechanism was coupled with one and two-dimensional models that simulated the fluid flow, heat and mass transfer in a rectangular channel where a solution of paraffin and oil flowed under laminar conditions. The test section used in the experiments was modeled in detail, and the numerical results were compared with the spatial distribution of the deposited wax for different times, until the steady state condition was reached. The model employed molecular diffusion was the only deposition mechanism. The comparison of experimentally and numerically obtained data

displayed large discrepancies in the transient deposition profiles, showing that the model under predicted the deposit thickness for the range of laminar Reynolds number investigated. The smaller deposit thicknesses predicted by the model were interpreted as an indication that deposition mechanisms other than molecular diffusion could be acting. It should be mentioned that the simulation work of Romero et al. (2006), did not solve the linear momentum equation for the flowing paraffin-oil solution. Instead, a locally, fully developed flow approximation was employed. In this approximation, knowing the mass flow through the channel, a fully developed flow profile is imposed at each axial coordinate, taking into account the decreasing of the flow cross section due to the growth of the deposited wax layer. It is conceivable that the discrepancy between measured and predicted deposition profiles verified can be partially attributed to the flow approximation employed, and not to the molecular-diffusion-based deposition model implemented. The present research was conducted with the objective of clarifying this issue,. Here, the equations governing the fluid flow of a Newtonian solution are solved, together with the equations governing the temperature and species concentration fields. As in the work of Romero et al., 2006, molecular diffusion was the only deposition mechanism implemented. As will be seen shortly in the results section, there are still appreciable differences between measured and predicted deposition profiles, with the simulations under estimating the deposit thicknesses.

2. MATHEMATICAL MODEL

As already mentioned, the main objective of the present research is to identify the relative importance of the wax deposition mechanisms proposed in the literature. To this end, in the present paper, a molecular diffusion model is analyzed, since this is the most widely accepted mechanism. The predictions are compared with experimental data obtained in the simple geometry employed in the experiments of Leiroz, 2004, and presented schematically in Fig. 1. The working fluid is a binary homogeneous solution of oil, the solvent, and wax, the solute. Oil enters the domain, which has a rectangular cross section (height a and width W), with constant mass flow rate, concentration and temperature. In the test section, water flows through channels connected to the upper and lower copper walls that form the channel, which has length equal to L. To obtain a fully developed flow condition at the copper wall, there is a plexiglass section at the entrance of the channel. A plexiglass section is also added downstream of the copper wall. Initially, water flows at the same temperature as the inlet oil, until an equilibrium state is obtained. The test begins, by reducing the water temperature T_{H2O} to a value below the wax appearance temperature for the solution, T_{WAT}. The deposition occurs when the oil temperature reaches a value lower than the wax appearance temperature, T_{WAT}. The wax deposition thickness is δ.

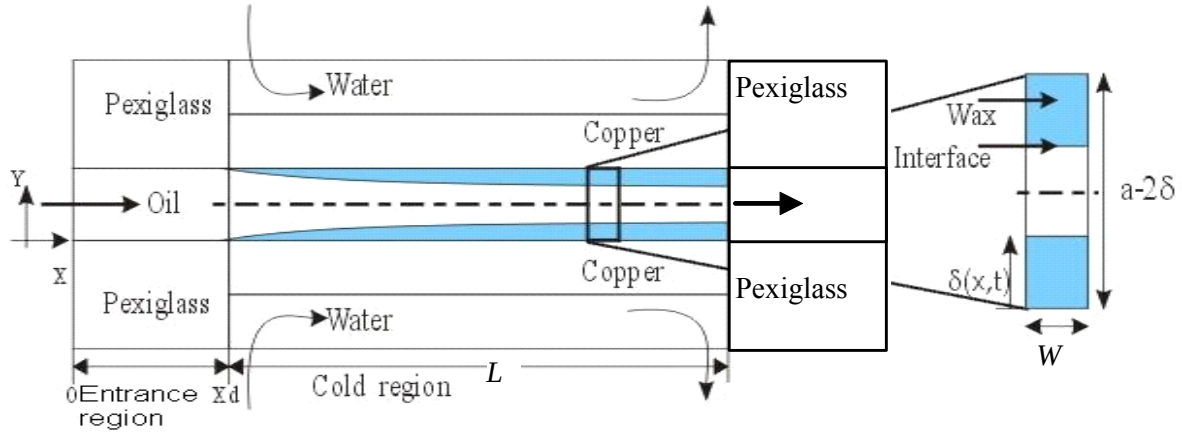

a) full domain b) side view

Figure 1. Schematic view of the test section.

To simulate the wax deposition process, a two-dimensional model was developed. The computational domain is shown in Fig. 2, where symmetry in relation to the horizontal axis was enforced. Since the heat loss to the ambient are expected to be small, the entrance and exit plexiglass regions were considered as adiabatic walls. Due to the high thermal conductivity of the copper, the test section wall temperature T_w was assumed constant and equal to the water temperature.

The oil mixture was considered as a Newtonian fluid with constant properties. The deposition is determined by the solution of the conservation equations of mass, momentum, energy and wax concentration. Due to the wax deposition process, the flow cross section area varies, thus the conservation equations are solved in a coordinate system that adapts to the geometry contour, (ξ, η), as shown in Fig. 2. When there is a border movement, the coordinate system presents a displacement velocity, $\mathbf{U_g} = u_g\,\mathbf{i} + v_g\,\mathbf{j}$, where the Cartesian components are $u_g = \partial x/\partial \tau$ and $v_g = \partial y/\partial \tau$.

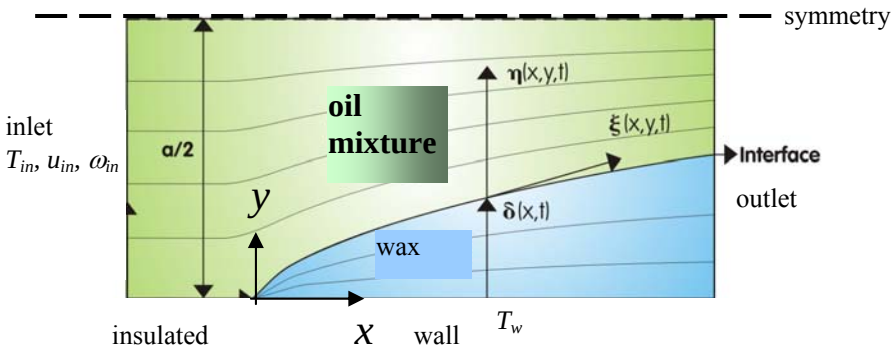

Figure 2. Computational domain and coordinate system.

The coordinate system adopted is such that $\vec{e}_\xi$ is tangent to the deposit interface and $\vec{e}_\eta$ .is aligned with the vertical direction, so that

$$\vec{e}_\xi = \frac{\partial \delta}{\partial x}\vec{e}_x + \sqrt{1-\left(\frac{\partial \delta}{\partial x}\right)^2}\,\vec{e}_y \;; \quad \vec{e}_\eta = \vec{e}_y \quad \text{and} \quad \xi = \frac{x - x_d}{x_c + x_d} \;; \quad \eta = \frac{y - \delta}{a/2 - \delta} \;; \quad \tau = t\,. \tag{1}$$

The conservation equations of mass and linear momentum for the liquid phase are

$$\mathbf{div}\ \tilde{\mathbf{U}} = 0 \;; \qquad \partial(\rho\,\mathbf{U})/\partial t + \mathbf{div}\left(\rho\,\tilde{\mathbf{U}}\,\mathbf{U}\right) = -\,\mathbf{grad}\ p + \mathbf{div}\,[\mu\ \mathbf{grad}\ \mathbf{U}\,] \tag{2}$$

where ρ and μ are the mixture density and absolute viscosity. p is the thermodynamic pressure, $\tilde{\mathbf{U}}$ represents the velocity vector relative to the (ξ, η) coordinates and **U** is the absolute velocity vector. These are related by $\tilde{\mathbf{U}} = \mathbf{U} - \mathbf{U_g}$, where $\mathbf{U_g}$ is the velocity vector due to the boundary movement. The concentration conservation equation is only solved at the liquid region and it is given by

$$\partial(\rho\,\omega)/\partial t + \mathbf{div}\left(\rho\,\tilde{\mathbf{U}}\,\omega\right) = \mathbf{div}\,[(\rho\,\mathcal{D}_{wax}\,)\ \mathbf{grad}\ \omega\,] \tag{3}$$

The properties of the liquid and solid phases were considered identical, therefore, the energy conservation equations for both liquid and solid regions are:

$$\partial(\rho\,T)/\partial t + \mathbf{div}\left(\rho\,\tilde{\mathbf{U}}\,T\right) = \mathbf{div}\,[(k/c_p)\ \mathbf{grad}\ T\,] \tag{4}$$

where k and c_p are the thermal conductivity and specific heat, and T is the temperature. Note that, because of the displacement of the coordinates, and the interface movement, it is necessary to introduce a convective term in the energy equation for the solid region, where **U** = 0.

To solve the set of equations (2), (3) and (4), the following boundary conditions were considered: uniform velocity u_{in}, temperature T_{in} and wax concentration ω_{in} at the inlet and negligible diffusion at the outlet. At the upper boundary a symmetry condition was defined. The energy equation is solved in the whole domain, thus a boundary condition at the lower boundary of the domain is needed. The entrance and exit wall regions were considered adiabatic, and constant temperature was specified at the copper test section wall. At the liquid-wax interface, continuity of heat flux and temperature are enforced. With respect to the flow equations, Eq. (2), no slip condition was imposed at the solid walls (inlet and exit wall regions and liquid-wax interface). The concentration boundary condition ω_{int} at the interface was specified from the known equilibrium oil-wax solubility curve whenever $T_{int} < T_{WAT}$, otherwise, the interface was considered impermeable (i.e., zero mass flux).

At the beginning of the process, the copper wall temperature is the same as the inlet oil-wax solution temperature. Thus, at t= 0, the interface temperature T_{int} is larger than T_{WAT}, therefore both δ and $d\delta/dt$ are zero. The growth of the deposited layer was accounted for by a molecular diffusion mechanism, as suggested by Burger et al. (1981). In this model, the deposition occurs when $T_{int} < T_{WAT}$ and the diffusion flux of wax toward the cold wall is estimated by Fick's law of diffusion,

$$\frac{\partial\, m_{wax}}{\partial\, t} = -\rho\ \mathcal{D}_{wax}\ W\ dx\ \left.\frac{\partial\ \omega}{\partial\ y}\right|_{int} \quad ; \quad m_{wax} = \rho_{wax}(1-\phi)\ W\ \delta\ dx \tag{5}$$

where ρ is the mixture density, $\mathcal{D}_{wax}$ is the molecular diffusion coefficient of the liquid wax in the solvent oil, ω is the concentration (or volume fraction of wax in the solution), m_{wax} is the wax mass deposited, ρ_{wax} is the solid wax density and $\phi=m/(m+m_{wax})$ is the porosity of the oil-filled wax deposit. $m=\rho\, W\, (a/2 - \delta)\, dx$ is the fluid mass contained in an elementary volume. Rearranging eq. (5), the wax deposition thickness can be obtained from,

$$\frac{\partial\, \delta}{\partial\, t} = -\frac{\rho}{\rho_{wax}} \frac{\mathcal{D}_{wax}}{(1-\phi)} \left.\frac{\partial\, \omega}{\partial\, y}\right|_{int} \tag{6}$$

3. NUMERICAL METHOD

The numerical method selected for solving the set of governing and auxiliary equations was the finite volume method (Patankar, 1980) with fully implicit time integration. The fluxes at the control volume faces were determined with the *Power-Law* scheme. The dependent variables in the linear momentum conservation equation were the contravariant velocity components (normal to the coordinate surface/line) (Pires and Nieckele, 1994), which were stored staggered from the scalar variables, to avoid oscillatory solutions. The pressure-velocity coupling was handled by an algorithm based on SIMPLEC (van Doormaal, and Raithby, 1984). The resulting algebraic system was solved by the TDMA line-by-line algorithm (Patankar, 1980) and a block correction algorithm was employed to speed convergence. The equations of conservation of mass, linear momentum and concentration were solved only in the liquid region. The energy equation was solved in the entire domain, in both solid and liquid regions.

In the resolution of phase change problems, the position of the interface is part of the solution, resulting in a more complex algorithm, since the size of the solid and liquid regions change with time. It is assumed that the movement of the fluid inside channel is not strongly influenced by the movement of the interface. Therefore, for each time interval, temperature, concentration and velocity fields can be solved maintaining a fixed solid/liquid interface.

Due to the interface movement, the computational mesh is generated each time the interface changes position. However, since the interface movement occurs only in the vertical direction, the horizontal mesh is maintained constant. The mesh is concentrated near the interface. The mesh distribution of 61 × 81 nodal points, in the vertical and horizontal direction, was defined based on grid tests. A comparison of the thickness of the deposit employing a mesh with 61 x 81 grid and 81 × 101 grid resulted in differences smaller than 2%. At the beginning of the process, 15 points are specified at the solid region, whose width is equal to 0.005 H. The final number of points in this region depends on the interface displacement. A time step of 10^{-8} seconds was specified. The convergence criterion consisted on requiring a residue inferior to 10^{-8} for all conservation equations.

4. RESULTS

The results obtained from the numerical solutions will now be presented and commented. Due to space limitations, only the most representative results will be presented.

Figure 3 presents the spatial and temporal distributions of the deposited wax obtained from the numerical solutions. In the figure, the abscissa represents the dimensionless axial coordinate of the channel, where the length of the active copper wall was chosen as the reference dimension. The ordinate represents the thickness of the deposited wax given in millimeters. The origin the axial coordinate is located at the beginning of the active copper wall. Due to this choice of origin, the adiabatic wall that represents the plexiglass wall in the experiments, positioned upstream of the copper wall, starts at a negative coordinate x = -1.4. The Reynolds number employed in the calculations presented was 366, and the solution had a Wax Appearance Temperature of 36.6 ^{o}C. These were the parameters utilized in the experiments conducted by Leiroz (2004). In fact, the calculations mimic all the geometric and flow characteristics of these experiments. In Figure 3, the symbols represent the experimental data from Leiroz (2004), while the solid lines are the predictions from the present calculations. The symbols and line colors represent different time intervals after the beginning of the cooling of the copper wall, and are cued to the legend in the figure.

An observation of the results presented in Figure 3 shows a reasonable agreement between measured and predicted wax deposition thicknesses for the steady state situation, specially if one takes into consideration the levels of experimental uncertainties reported by Leiroz (2004). However, the same level of agreement between experiments and simulation is not obtained for the transient cases shown in the figure. Indeed, the discrepancies are larger for shorter time intervals measured after the start of cooling. For each time interval shown in the figure, a similar trend is observed. There is a very good agreement up to a certain axial position in the channel, after which the measured deposit thicknesses continue to grow, while the predictions indicate a decrease in deposition. It is interesting to note that the axial positions at which experiments and computations diverge increase with time, indicating a better agreement for higher values of the time interval, up to the steady state configuration already commented, which displays the best level of agreement of all data sets.

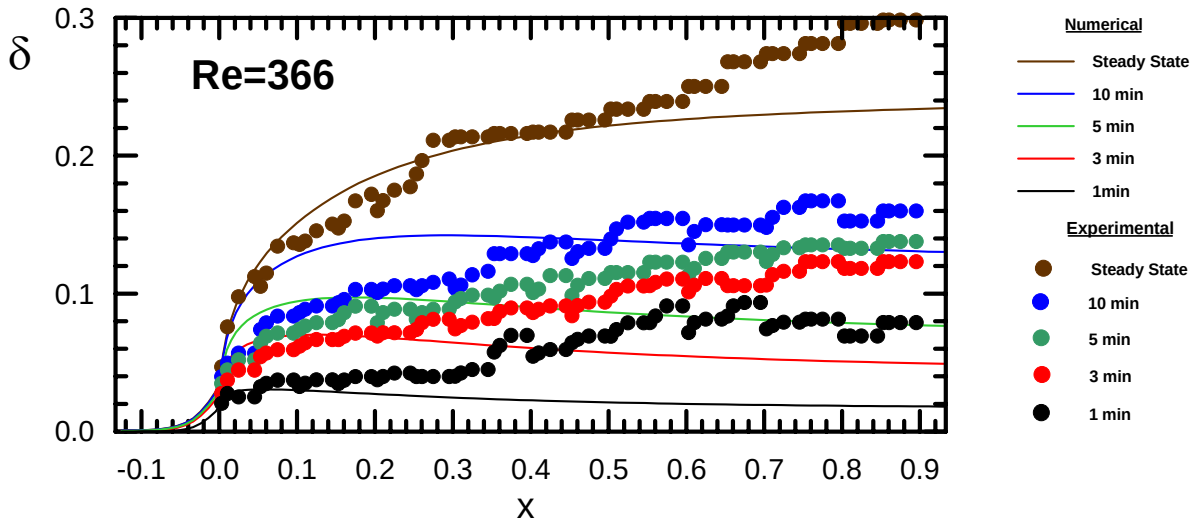

Figure 3 – Comparison of measured and predicted transient wax deposition profiles for Re = 366 and WAT = 36.6°C

The trends displayed by the deposition profiles predicted by the numerical simulation and presented in Figure 3, seem to be physically plausible and in agreement with the expected behavior for the molecular diffusion deposition model adopted. Indeed, it is expected that after the start of the cooling process, strong cross stream temperature gradients would prevail at the axial position where the copper wall begins, i.e, at around X =0. This is due to the relatively thinner thermal boundary layer at this position. Since the solubility of the wax is a decreasing function of temperature, a sharp concentration gradient is developed at this location, leading to a higher flux of wax toward the wall. As the flow develops along the channel, smaller temperature and concentration gradients are expected, producing relatively smaller wax diffusive fluxes toward the wall. These trends can be verified in the temperature profiles presented in Figure 4. In this figure temperature profiles for three axial coordinates are presented superimposed to the wax deposition profiles. Each figure corresponds to a time interval after cooling of the wall starts, respectively, at 1 minute, 3 minutes and at the steady state condition, after which the interface no longer grows. It can be verified that, for each time interval, the temperature gradients decrease for higher values of the channel axial coordinate. Also, a comparison of the relative magnitudes of the temperature gradients for the same axial positions and different times, indicate that the gradients are less steep as the steady state is approached. This leads to decreasing mass fluxes toward the wall, as can be verified by the concentration gradients presented in Figure 5, for the same positions and times presented for the case of Figure 4.

The fact that measured and predicted deposition profiles deviate beyond a certain value of the channel axial coordinate, even though the predictions seem to be physically plausible as discussed above, could be an indication that the molecular-diffusion-based deposition mechanism adopted in the simulation might not be adequate. Indeed, it is seen that the measured deposition thicknesses tend to be always larger than the predicted ones. This could be attributed to the action of deposition mechanisms other than molecular diffusion.

A second look at the temperature profiles presented in Figure 4 lends support to this assumption. In each temperature profile presented in Figure 4, an auxiliary vertical line was drawn at the value 36.6°C, representing the wax appearance temperature – WAT – for the fluid studied. For the case of 1 minute after the initiation of the cooling of the wall shown in Figure 4(a), it can be verified that a portion of the fluid close to the wax deposit is below the WAT for all three axial positions depicted in the figure. Further, it can also be seen that the region of temperature below the WAT increases in size for axial positions further downstream into the channel. For longer time interval after cooling, the regions of temperatures below the WAT are less pronounced, as can be seen in Figure 4(b). At steady state, Figure 4(c), the regions of temperature below the WAT are not present. An observation on the deposition results presented in Figure 3, shows that there might be a relationship between the magnitude of the regions of temperature below the WAT and the departure of the experimental data from the predictions. It is conceivable that the degree of sub-cooling necessary for the nucleation of wax crystals in the flowing solution is attained at these regions close to the deposit surface, leading to the formation of suspended crystals that might be aggregated to the deposit due to a lateral transport mechanism such as Brownian diffusion. A model for wax crystal formation accompanied by a Brownian diffusion deposition model is presently being incorporated in the simulation developed. At the time of preparation of this text, no results were yet available.

The numerical solutions obtained also provided information on the velocity profiles along the channel length. These are presented in Figures 6(a) – (c). A careful analysis of the three figures allows the observation of an acceleration of the velocity profile induced by the decrease in flow area due to the wax deposition, what precludes the

attainment of a fully developed flow condition. This acceleration is much more pronounced for the steady state case where the deposited wax layer is more significant.

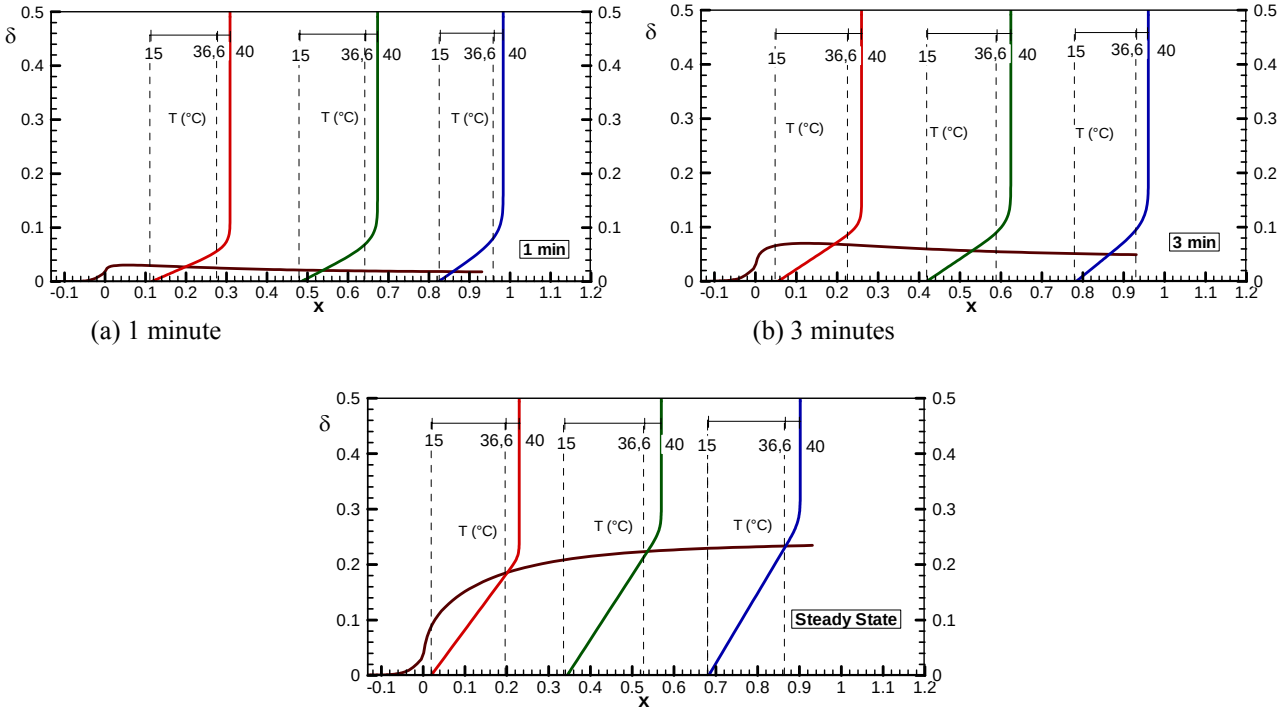

(a) 1 minute (b) 3 minutes

(c) steady state

Figure 4 – Temperature profiles at three channel axial positions for different time intervals after start of cooling, for Re = 366 and WAT = 36.6°C. (a) 1 minute, (b) 3 minutes, and (c) steady state.

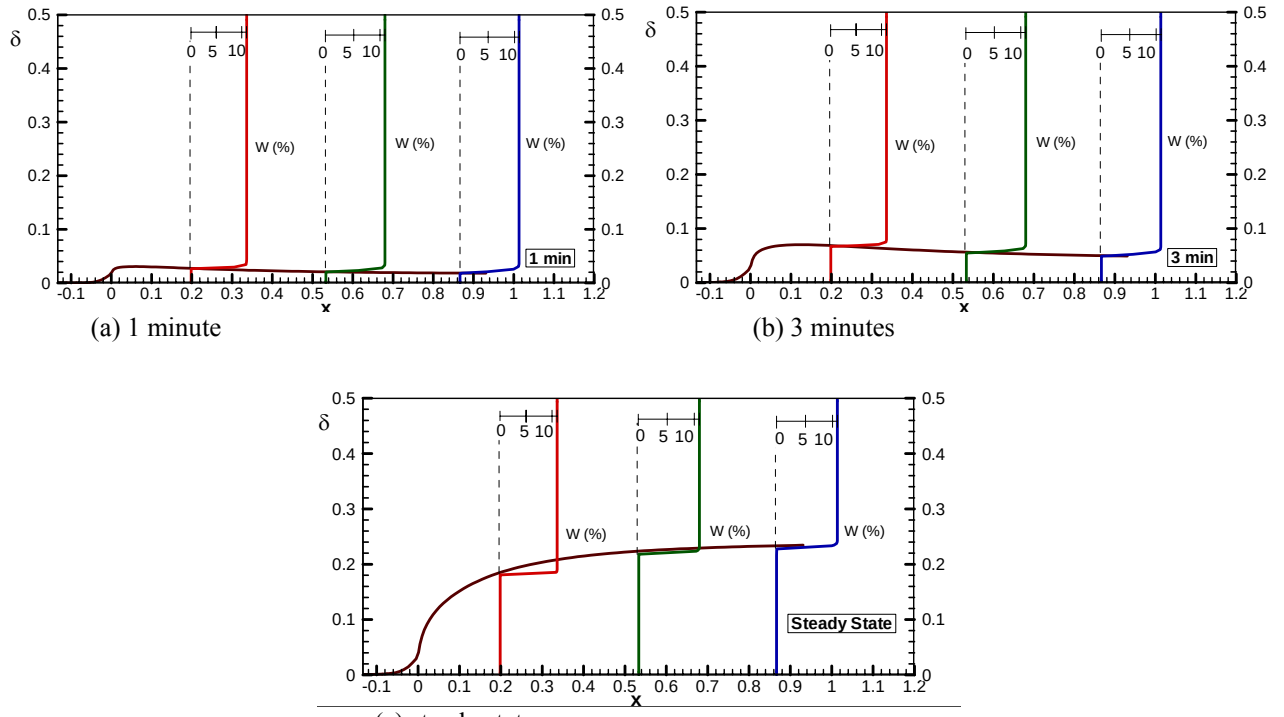

(a) 1 minute (b) 3 minutes

(c) steady state

Figure 5 – Wax concentration profiles at three channel axial positions for different time intervals after start of cooling, for Re = 366 and WAT = 36.6°C. (a) 1 minute, (b) 3 minutes, and (c) steady state.

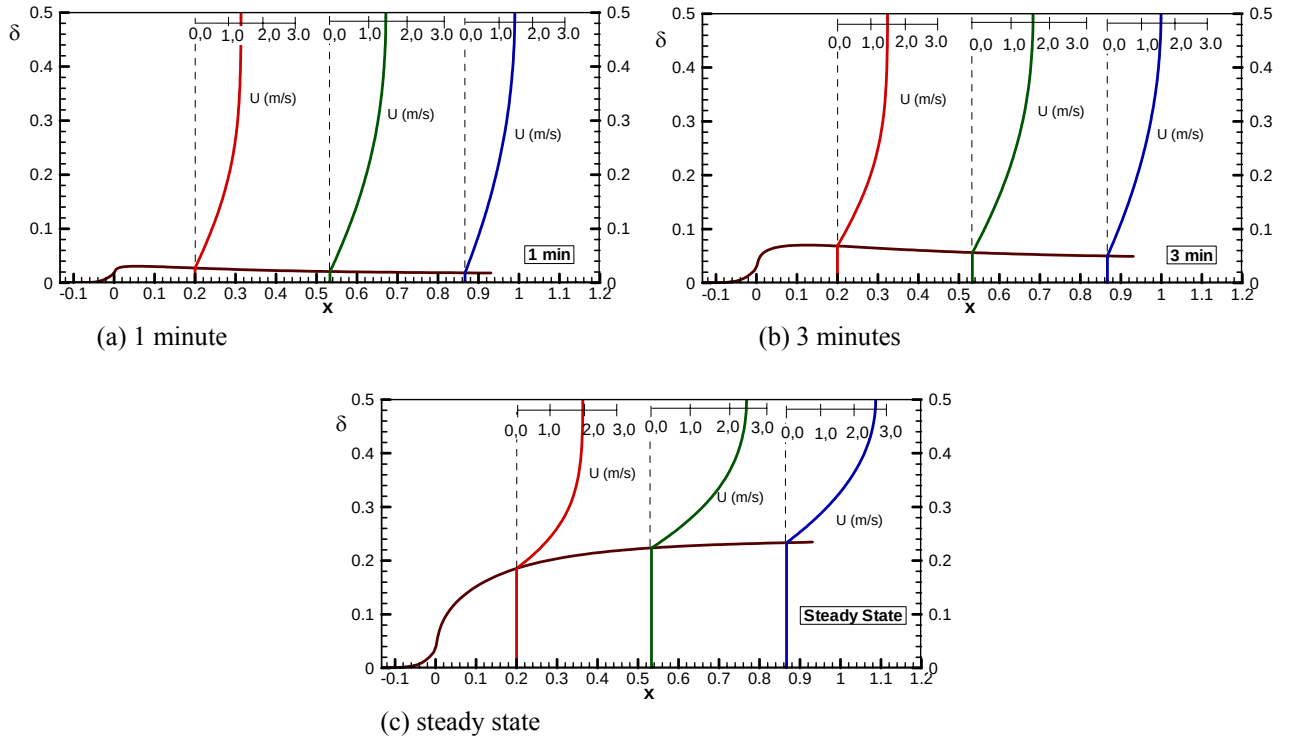

(a) 1 minute (b) 3 minutes

(c) steady state

Figure 6 – Axial velocity profiles at three channel axial positions for different time intervals after start of cooling, for Re = 366 and WAT = 36.6°C. (a) 1 minute, (b) 3 minutes, and (c) steady state.

5. CONCLUDING REMARKS

The present paper presented the results of an ongoing research program aimed at simulating the deposition of wax at the inner walls of channels. In particular, attention was focused on the evaluation of the relative importance of the deposition mechanisms. To this end, a simulation model was developed in which the equations governing the conservation of mass, linear momentum, energy and chemical species were solved numerically. Wax deposition and the deposit growth were modeled by employing molecular diffusion as the only deposition mechanism. The geometry, boundary and initial conditions of the simulation mimic a configuration previously studied experimentally in the laboratory.

A comparison of measured and predicted transient deposition profiles revealed a reasonable level of agreement for the steady state configuration. However, the predicted transient profiles deviated from the measured data. The deviations were more pronounced for profiles taken at small time interval after the initiation of the cooling of the channel wall. Also, for the same time interval, the deviations were seen to increase for larger values of the channel axial coordinate.

The deviations between measured and predicted deposition profiles were observed even though the behavior of the numerical solutions was shown to be physically plausible and compatible with the molecular-diffusion-based deposition model adopted, and the experiments were believed to be reliable. The deviations were attributed to the action of other deposition mechanism acting in addition to molecular diffusion. Observation of detailed data on temperature and concentration profiles produced by the numerical solutions revealed regions of fluid close to the deposit interface where the temperature was below the wax appearance temperature for the solutions. These regions were more pronounced for small time intervals after initiation of cooling, and for positions with larger values of the axial coordinate. It was proposed that at these regions of sub-cooled fluid could be the site of wax crystal formation that would, possible be driven toward the wall by a Brownian-diffusion-based mechanism contributing, thereby, for the larger thicknesses of deposited wax observed in the experiments.

Observations of the velocity profiles produced by the simulation model indicate that the acceleration induced by the decreased flow area due to the growth of the deposit layer precludes the attainment of a fully developed flow condition.

6. ACKNOWLEDGEMENTS

The authors gratefully acknowledge the support awarded to this research by the PETROBRAS Research Center – CENPES, the Brazilian Research Council – CNPq and the Fund for Research and Development in Petroleum – CTPetro.

7. REFERENCES

Brown,T.S, Niesen, V.G. and Ericckson, D.D., 1993, "Measurement and Prediction of the Kinetics of Paraffin Deposition", 68th Annual Conference of the Society of Petroleum Engineers paper no. SPE 26548.

Burger, E.D., Perkins, T.K. and Striegler, J.H., 1981, "Studies of Wax Deposition in the Tras Alaska Pipeline", Journal of Petroleum Technology, June, 1075-1086.

Fusi, L., 2003, "On the Stationary Flow of a Waxy Crude Oil with Deposition Mechanisms", Non Linear Analysis, 53, 597-526.

Leiroz, A.T., 2004, "Study of Wax Deposition in Petroleum Pipelines", Ph.D. thesis, Pontifícia Universidade Católica do Rio de Janeiro – PUC-Rio, Rio de Janeiro, Brazil (in portuguese).

Romero, M.I., Leiroz, A.T., Nieckele, A.O. and Azevedo, L.F.A., 2006, "Evaluation of a Diffusion Based Model to Predict Wax Deposition in Petroleum Pipelines", 13th International Heat and Mass Transfer Conference, Sidney, Australia.

Patankar, S. V., 1980, “Numerical Heat Transfer and Fluid Flow”, McGraw-Hill.

Pires, L. F. G. and Nieckele, A. O., 1994, “Numerical Method For The Solution Of Flows Using Contravariant Components In Non-Orthogonal Coordinates”, Proceedings of the V Brazilian Meeting on Thermal Sciences, SP, pp. 343-346 (in Portuguese).

van Doormaal, J. P. and Raithby, G. D., 1984, “Enhancements of the Simple Methods for Prediction Incompressible Fluid Flow,” Numerical Heat Transfer, 7, pp. 147-163.

8. RESPONSIBILITY NOTICE

The authors are the only responsible for the printed material included in this paper.